Conference paper

OPTO-ELECTRONICS REVIEW 7(2), 81–86 (1999)

Intersubband transitions in n-type quantum well systems*

M. ZAŁUŻNY*

Institute of Physics, Maria Curie-Skłodowska University,
1 M. Curie-Skłodowska Sq., 20-031 Lublin, Poland

Specific properties of intersubband transitions in n-type semiconductor quantum well structures are reviewed. Some interesting aspects of coupling of infrared radiation with intersubband transition in multiple quantum well structures are also considered. Recent achievements in intersubband emission are then discussed with specific emphasise on the quantum cascade lasers.

Keywords: quantum wells, intersubband transitions, semiconductor lasers

1. Introduction

The success of various epitaxial growth technique such as molecular-beam epitaxy, vapor-phase epitaxy, and chemical vapor deposition techniques has made it possible to grow high-quality multilayer semiconductor structures with composition and doping controlled down to a single monolayer. When different semiconductors adjoin there will be, in general, discontinuities of the conduction-band and valence-band edges. These discontinuities are source of the carrier confinement. In the best-investigated case $Al_xGa_{1-x}As$/$GaAs$/$Al_xGa_{1-x}As$ system, both electrons and holes can be confined in the GaAs layer (see Fig. 1). Owing to the strong confinement of the free carriers in the small size regions, size quantization produces two-dimensional (2D) subbands [or minibands in the case of superlattices (SLs)]. This affects dramatically the optical properties of the above systems in IR region. It is well known that in a bulk crystal the intraband optical transitions within the same band are forbidden and may only be induced by phonons or impurities to provide the momentum conservation. In the case of 2D systems momentum conservation in the growth direction is relaxed. Consequently, the optical transitions between different subbands are possible (see Fig. 1).

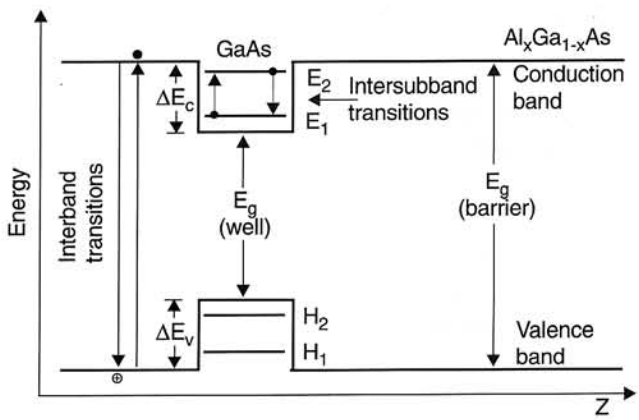

Fig. 1. Schematic band diagram of a GaAs/AlGaAs quantum well. Intersubband transitions between electrons levels E_1 and E_2 are indicated. Conventional interband transitions take place between the conduction and valence bands.

In this paper the basic properties of the intersubband transitions (ISBTs) in n–type quantum well systems will be discussed. A brief review of the progress in the practical applications of ISBTs in the infrared emitters concentrating on the so-called quantum cascade (QC) laser will also be presented.

Information on other interesting infrared quantum well devices based on the ISBTs such as infrared detectors can be found in Ref. 1.

* e-mail: zaluzny@tytan.umcs.lubin.pl

* The paper presented there appears in SPIE Proceedings Vol. 3725, pp. 157–163.

2. Intersubband absorption

The quantum well can be treated in the first approximation as a well-known particle-in-a-box problem. Thus, the positions of energy levels, the "subbands" are determined by the height ΔE_c and width (L_{QW}) of the well. For infinitely high barriers and parabolic bands the intersubband transition energy between the lowest (E_1) and first excited state (E_2) in conduction band is given by $E_{21} = 3\hbar^2\pi^2/2m^*L_{QW}^2$, where m^* is the (isotropic) electron effective mass in the quantum well. Consequently, by tailoring the quantum well structure, it should be possible to achieve the situation when photon energy $\hbar\omega$ coincides with E_{21}. The matrix element connected with optical transitions between i and j subbands can be written (in the envelope function approximation) in the following form $\langle j|\vec{\varepsilon}\cdot\vec{r}|i\rangle = \sin(\theta)z_{ij}$, where $z_{ij} \equiv \langle\phi_j|z|\phi_i\rangle$, ϕ_j is the envelope function for j-th subband in the z (confinement) direction, $\vec{\varepsilon} \equiv (\cos(\theta), 0, \sin(\theta))$ is the polarization vector of an incident light and φ is the angle between the direction of incident light and the direction perpendicular to the layer.

In the case infinitely deep quantum well $z_{21} \cong 0.18L_{QW}$. Thus, the oscillator strength of the intersubband transitions between ground and first excited state writes

$$f_{12} = \frac{2m^*E_{21}}{e^2\hbar^2}z_{21} \approx 0.96 \qquad (1)$$

where e is the electron charge. As it can be seen the oscillator strength corresponding 1→2 intersubband transitions is close unity.

West and Eglash [2] were the first who demonstrated intersubband transitions in $GaAs/Al_xGa_{1-x}As$ multiple quantum well (MQW) systems (electrons were introduced by doping the barrier materials.) They found, in accordance with theoretical prediction, that the oscillator strength connected with these transitions was large (close unity) and had only one nonzero component (along the growth direction). This means that the optical electric field must have a component parallel to the growth direction in order to induce the intersubband absorption in conduction band of quantum well with isotropic effective mass. In plane polarized transitions can be observed in systems with anisotropic effective mass. The above type of transitions can also be observed in the valence band due to strong subband mixing effect. ISBTs have now been observed in many other material systems. Various 2D confinement potentials have been investigated including step quantum wells and coupled quantum wells [1].

The main properties of intersubband absorption spectra of a single quantum well (SQW) can be described using the one electron picture. However, the quantitative description of the absorption line shape has to take into account the influence of Coulomb interaction on the electron energy spectrum (band banding effect) and intersubband transitions (resonant screening effect) particularly when surface electron concentration is large ($N_s \geq 10^{12}$ cm^{-2}). The above mentioned interaction is usually studied using mean-field approach [3].

The quantum well thickness L_{QW} is much smaller than the wavelength of IR radiation. The Fermi wave vector is several orders of magnitude larger than the parallel component of the photon wave vector. Thus, the external perturbation (incident radiation field) inducing ISBTs can be taken in the following form $E^{ext}(t) = E^{ext}(\omega)\exp(-i\omega t)$ [we neglect here for simplicity the small difference between the dielectric constant of the well material (ε_w) and barrier material (ε_b)].

When the radiation is polarized in the x – z plane the optical absorption per unit area of SQW can be approximated by [3]

$$P_{SQW}(\omega) = \frac{1}{2}\mathrm{Re}\int_{-\infty}^{\infty}\vec{j}(z,\omega)\vec{E}^*(z,\omega)dz = \frac{1}{2}\sum_j \mathrm{Re}[\tilde{\sigma}_{jj}^{(2D)}(\omega)|E_j^{ext}(\omega)|^2] \qquad (2)$$

where $j(z,\omega) = [j_x(z,\omega), 0, j_z(z,\omega)]$ is the Fourier component of the current density induced in SQW and $\vec{E}(z,\omega)$ is the total electric field in the system.

The modified 2D conductivity $\tilde{\sigma}_{jj}^{(2D)}(\omega)$ defined by

$$\tilde{\sigma}_{jj}^{(2D)}(\omega) = \frac{1}{E_j^{ext}(\omega)}\int_{-\infty}^{\infty}dz j_j(z,\omega) = \frac{j_j^{(2D)}(\omega)}{E_j^{ext}(\omega)} \qquad (3)$$

describes the response of the electron gas on the j-th component of the external electric field $\vec{E}^{ext}(\omega)$.

At this point it is interesting to note that due to the presence of ISBTs $E_x(z,\omega) \cong E_x^{ext}(\omega)$ but $E_z(z,\omega) \cong E_z^{ext}(\omega) + 4\pi i\omega j_z(z,\omega)$.

The expression for $\tilde{\sigma}_{zz}^{(2D)}(\omega)$ resulting from the time-dependent local density approximation takes form [3]

$$\tilde{\sigma}_{zz}^{(2D)}(\omega) = \Lambda\frac{-i}{[\tilde{E}_{21}^2 - (\hbar\omega)^2]/2\hbar\omega\Gamma - i} \qquad (4)$$

where

$$\Lambda = N_s e^2 f_{12}\hbar/2m^*\Gamma,\ \tilde{E}_{21} \equiv \hbar\tilde{\omega}_{21}(> E_{21})$$

is the intersubband transition energy modified by the depolarization and exciton-like effects, $\tau = \hbar/\Gamma$ is the dephasing time connected with 1→2 transitions and E_{21} is the intersubband spacing calculated including the band bending effect. In this paper we restrict to the two parabolic subband models with only ground subband occupied.

We find that in the above model the resonant screening leads only to the blue-shift of the intersubband resonant energy. However, when the subband separation depends on the parallel component of the electron wavevector ($k_{||}$) the resonant screening leads to the more complicated deformation of the absorption line shape [4].

The parallel (intrasubband) conductivity appearing in Eq. (2) can be approximated by the Drude-like expression $\tilde{\sigma}_{xx}^{(2D)}(\omega) = N_s e^2/m^* (\tau_{||}^{-1} - i\omega)$, where $\tau_{||}(> \tau)$ is the intrasubband relaxation time.

From Eq. (2) we find that the absorptance (= the fraction of the incident energy absorbed) of SQW surrounded by semi-infinite barriers is given by

$$\begin{aligned} A_{SQW}(\omega,\theta) &= A_{SQW}^{\perp}(\omega,\theta) + A_{SQW}^{||}(\omega,\theta) \\ &= \frac{4\pi}{c\sqrt{\varepsilon_w}} \mathrm{Re}\,\tilde{\sigma}_{zz}^{(2D)}(\omega)\tan(\theta)\sin(\theta) \\ &+ \frac{4\pi}{c\sqrt{\varepsilon_w}} \mathrm{Re}\,\tilde{\sigma}_{xx}^{(2D)}(\omega)\cos(\theta) \end{aligned} \tag{5}$$

Taking for estimations $\tilde{E}_{21}/2\Gamma \approx 10$ one finds that $\mathrm{Re}[\tilde{\sigma}_{zz}^{(2D)}(\omega)/\tilde{\sigma}_{zz}^{(2D)}(\omega)] \approx \tau\tau_{||}\tilde{\omega}_{21}^2 f_{21}/2 \sim 200$. Thus, the relative contribution of the intrasubband transitions to $A_{SQW}(\omega,\theta)$ is vanishingly small except the case of nearly normal incidence.

In the two-subband limit we have

$$\begin{aligned} A_{SQW}^{\perp}(\omega) &= \frac{4\pi}{c\sqrt{\varepsilon_w}} \mathrm{Re}\,\tilde{\sigma}_{zz}^{(2D)}(\omega) = \\ &= \overline{A} \frac{1}{\{[\tilde{E}_{21}^2 - (\hbar\omega)^2]/2\hbar\omega\Gamma\}^2 + 1} \end{aligned} \tag{6}$$

where $\overline{A} = 4\pi\Lambda/c\sqrt{\varepsilon_w}$. Taking the typical for GaAs values of $m^* = 0.066\ m_0$ and $\varepsilon_w = 10.9$ we find that $\overline{A}_{|GaAs} \cong 0.016 \times f_{12} N_s [10^{11}\ cm^{-2}/\Gamma\ meV]$.

As revealed by the geometrical factor $\sin^2(\theta)/\cos(\theta)$ in Eq. (5) care must be taken when choosing the experimental configuration in order to ensure a good coupling efficiency of the light with ISBTs. Some of usual configurations are sketched in Fig. 2. When the light is incident at Brewster's angle, the coupling efficiency is rather small and a large number of QWs is required to get significant absorption [2]. The multi-pass

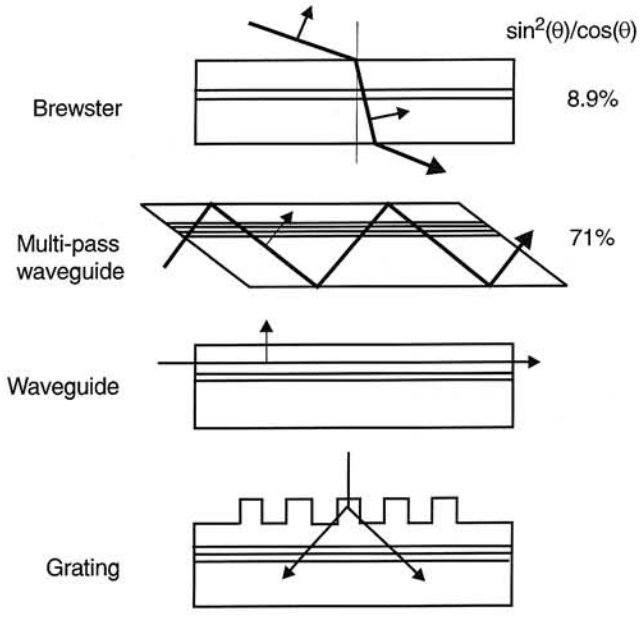

Fig. 2. Experimental configurations for observing ISBTs. Quantum efficiency is indicated.

waveguide configuration [total internal reflection (TIR) geometry], where the light enters the sample (usually) at normal incidence on a facet polished at 45° angle, is widely used for spectroscopic measurements since it allows large absorption due to the excellent coupling of p-polarized light to multipasses within the active layer. In the waveguide configuration absorption of light propagating with a polarization perpendicular to the layer plane (TM mode) can be made arbitrary large by adjusting the waveguide length. The grating configuration which consists of a linear or crossed grating fabricated on top of the sample, is mainly used for quantum well detectors since it allowes normal incidence irradiation [1].

In all experimental papers employing the Brewster angle geometry, analysis of IR spectra of multiple quantum well (MQW) structures is performed by application of Beer's law (the travelling wave approximation). This approximation is equivalent to neglecting effects induced by multiple reflections in the MQW structure itself and in the substrate. It leads to the following relation between $A_{SQW}(\theta,\omega)$ and the absorptance of MQW structure [1]:

$$\begin{aligned} A_{SQW}(\theta,\omega) &= 1 - [1 - A_{SQW}(\theta,\omega)^N] \\ &= 1 - \exp\{N \ln[1 - A_{SQW}(\theta,\omega)]\} \\ &\cong 1 - \exp[-N A_{SQW}(\theta,\omega)] \end{aligned} \tag{7}$$

where N is the number of the quantum wells in the system. Writing the above equation we have employed the fact that $A_{SQW}(\theta,\omega) \ll 1$. In the case of typical Brewster angle geometry such approach has a good jus-

tification. Because the external angle of incidence in this geometry is close to the Brewster angle, the phase-matched interference effects in the substrate are negligible. Moreover, the small value of the refraction angle ($\theta \approx 17°$ for GaAs) makes the coupling of IR radiation to intersubband transitions weak and consequently effects connected with multiple reflections (electromagnetic coupling) between different QWs are also negligible. Many authors (e.g., Ref. 1) try to employ the travelling wave approximation also in the case of TIR geometry. Such approach is very questionable. The role of multiple reflections (inside the MQW structure) is enhanced since the internal angle of light propagation (θ_{tir}) is now substantially larger than in the case of Brewster angle geometry (usually $\theta_{tir} = 45°$ or it is even larger). Moreover, the interference between the incident and reflected light at the semiconductor-air or semiconductor-metal interface (the standing wave effect) modifies substantially the spatial distribution of the normal component of the electric field of IR radiation. In our recent paper [5] we have discussed the above problem employing the effective medium approach. In this approach the MQW structure has optical characteristics of a uniaxial material. The components of the dielectric tensor describing the effective medium can be written in terms ε_b, ε_w and $\tilde{\sigma}_{jj}^{(2D)}(\omega)$. Numerical results presented in Ref. 5 indicate that when angle of incidence is not large (< 45°) the electromagnetic coupling between QWs can be neglected. The standing wave effect can be included replacing, in the travelling expression (6) the single quantum well absorptance $A_{SQW}^{\perp(\parallel)}(\theta,\omega)$ by the effective absorptance $\overline{A}_{SQW}^{\perp(\parallel)}(\theta,\omega) = A_{SQW}^{\perp(\parallel)}(\theta,\omega)\left\langle E_{z(x)}^2\right\rangle / (E_{z(x)}^+)^2$, where $E_{z(x)}^{(+)}$ is the amplitude of the z(x) component of the electric field of the incident light, $E_z(x)$ is the z(x) component of the electric field in the structure calculated taking $\varepsilon_{jj}(\omega) = 0$ and $\varepsilon_w = \varepsilon_b$. Symbol $\langle \ldots \rangle$ denotes averaging over the region occupied by MQWs. However, when the angle of incidence is large and the structure contains large number of QWs multiple reflections between different QWs start to play important role. Preliminary experimental results [6] seem to support the above suggestion. It is interesting to note that the correct description of this coupling must taken into account even the small difference between the dielectric constants of the well and barrier materials.

3. Intersubband emission

Now we discuss the application of ISBTs in semiconductor diode lasers working in the infrared. When appropriate electric field is applied across a weakly tunnelling MQW, the ground level $E_1(n)$ of the n-the quantum well can be brought almost or exactly on resonance with the second level $E_2(n+1)$ of the (n+1)-th quantum well. In such a case, electrons in the $E_1(n)$ level can flow into $E_2(n+1)$ and then relax to the $E_1(n+1)$ level (we assume that thickness of the barrier is sufficiently small). Some time ago, Kazarinov and Suris considered such a cascade transport for the first time [7] and pointed out that it may lead to the emission of infrared radiation. They have shown that the emission should occur if $E_1(n)$ is biased slightly above $E_2(n+1)$. Although quite weak, the predicted infrared radiation was detected by Helm et al. [8]. Unfortunately, the observation of the intersubband emission is difficult because of the non-radiative processes. For intersubband energies well below the optical phonon energy ($\lambda > 35$ μm), the nonradiative relaxation between the subbands is dominated by the relatively slow emission of acoustic phonons. At energies larger than the optical phonon energy the emission of LO-phonons reduces substantially the lifetimes of electrons in the excited subbands. In the case GaAs QWs non-radiative lifetime (τ_{ph}) connected with LO-phonon emission (acoustic-phonon emission) ranges from ≈ 0.3–2 ps (≈ 100–400 ps). However, the radiative lifetime (τ_r) is rather long. It exhibits a $\lambda^2 m^*$ evolution. Typical values of τ_r in GaAs QWs are of the order of 15 ns at $\lambda = 4$ μm and 9 μs at $\lambda = 100$ μm. Thus, the balance between the radiative and non-radiative processes is not favorable for spontaneous emission. Consequently, we cannot expect high efficiency of the light emitting devices based on ISBTs. Nevertheless, if population inversion can be achieved between the subbands, large stimulated gains are expected because of the large value of the corresponding oscillator strength. The condition for population inversion requires the non-radiative lifetime in the upper subband to be longer than in the lover subband. In tunnelling structures, this condition is equivalent the necessity to both provide a high injection current density and quickly remove electron from the ground subband with a time shorter than τ_{ph} of the excited subband. Several refined geometries have been proposed to fulfil the above mentioned conditions.

3.1 Quantum cascade laser

Intersubband luminescence has effectively been observed in coupled QW structures by a group of scientists at AT&T Bell Laboratories [9]. They reported an intersubband laser action at wavelength of 4.2 μm by feeding the current of about 1 A (≈ 15 kAcm^{-2})

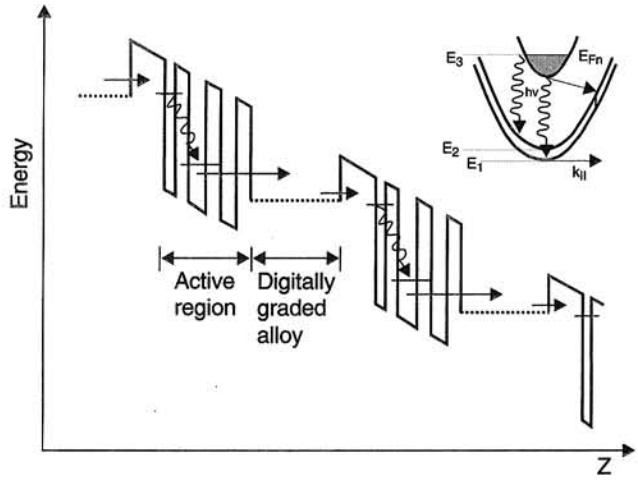

Fig. 3. Conduction band energy diagram of a portion of the 25-period (active region plus injector) section of the quantum cascade laser grown by MBE with the $Al_{0.48}In_{0.52}As/Ga_{0.47}In_{0.53}As$ heterojunction materials. The insert shows schematic representation of the dispersion of n = 1,2 and 3 states parallel to the layers. The wavy arrows indicate the laser transitions. The straight arrows represent the intersubband optical phonon processes.

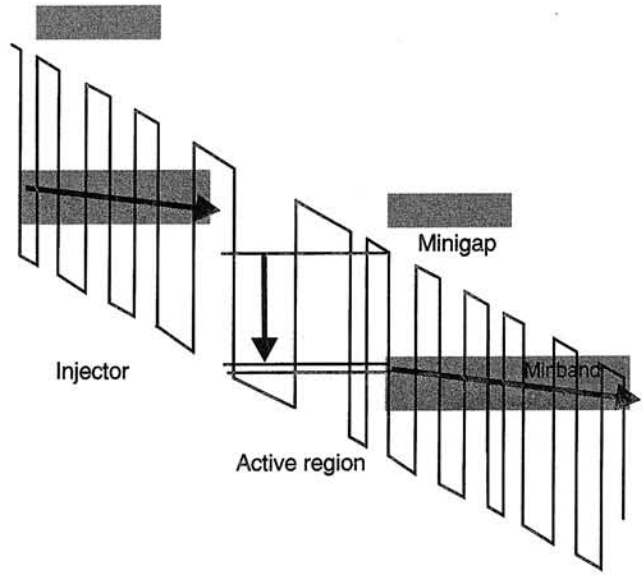

Fig. 4. Schematic energy diagram of a portion of QC laser with vertical emission.

through 25 periods of a novel InGaAs/InAlAs triple quantum well structure (see Fig. 3).

Each period of this structure contains an n-type injector layer and three coupled quantum wells with thicknesses 0.8 nm, 3.5 nm and 2.8 nm, respectively, separated by 3.5 nm barrier. The injector layer consists of a graded gap pseudoquaternary alloy. The graded gap varies from lower to higher values in going from left to right in each period. Consequently, at zero applied bias, the band diagram of the structure has an overall sawtooth shape. When a bias voltage of about 350 meV is applied across an each period, electrons are first injected through a tunnel barrier into the n = 3 state and then relaxed by emission of optical phonons. However, a small fraction (0.1–0.03%) emits also photons. To achieve light amplification QWs are designed so that the n = 3 state is more populated than the lover one (n = 2); the role of the n = 1 state is to siphon electrons fast enough out of the n = 2 level into the "injector" region. The whole structure is embodied in an infrared waveguide. Pulsed operation was achieved up to 125 K and the threshold current density was found to vary exponentially with temperature [$\exp(T/T_0)$] from 6.0 kA/cm^2 at $T_0 \approx 112$ K. Peak powers as large as 32 mW were obtained. The luminescence peak of the structure in Fig. 3 is relatively broad full-width at half-maximum (FWHM) ≅ 15 meV due to the interface roughness and the impurity distribution. As a consequence the peak material gain is reduced.

To alleviate this problem the structure with the double quantum well (with "vertical transitions") was design [10]. As such this transition should be less sensitive to interface roughness since the number of interfaces involved in the optical transition are now only two instead of the four involved in the previous ("diagonal") one. This considerably reduced the width of the luminescence spectrum (FWHM ≅ 7.5 meV). To prevent electron escape into the continuum (a problem which is less sensitive in the case of the diagonal transitions), the superlattice of the digitally graded injector is now designed as an effective Bragg reflector for electrons in higher excited (n = 3 level) and to continuously ensure swift electron escape from the lover states as in the previous structure (see Fig. 4). The levels 1 and 2 are separated by optical phonon energy. The threshold current is comparable for the two structures. CW operation has been achieved for the above type of structure up to a heat sink temperature in excess of 100 K for wavelengths between 4 and 8.5 μm and up to 50 K between 9 and 12 μm. An important factor in achieving CW operation has been used of an InP substrate as the lower waveguide cladding region rather than an AlInAs layer since the latter alloy has ~ 20 times larger thermal conductivity than InP. In the waveguide design the confinement was enhanced using the electromagnetic surface waves (surface plasmon) of a metal-semiconductor interface directly above the active region of the laser.

More recently the design of vertical transitions QC laser has been further improved (for details see Ref. 10). The group at AT&T Bell Laboratories has achieved room temperature pulsed operation in the 8–12 μm wavelength range. The above mentioned devices are the first semiconductor lasers working at room temperature in the mid-infrared. They have variety of potential use including night vision, pollution monitoring, industrial process control, collision avoided radars in automobiles or point-to-point communications.

At the end we note that very recently Bell Laboratories group reported dual-wavelength emission from optically cascaded intersubband transitions [11].

References

1. B.F. Levine, "Quantum-well infrared photodetectors", *J. Appl. Phys.* **74**, R1–R81 (1993).
2. L.C. West and S. J. Eglish, "First observation of extremely large dipole infrared transition within the conduction band of a GaAs quantum well", *Appl. Phys. Lett.* **46**, 1156–1157 (1985).
3. T. Ando, A. Fowler, and F. Stern, "Electronics properties of two dimensional systems", *Rev. Mod. Phys.* **54**, 437 (1982).
4. M. Załużny, "Intersubband absorption line broadening in semiconductor quantum wells: Nonparabolicity contribution", *Phys. Rev.* **B43**, 4511–4514 (1991).
5. M. Załużny and C. Nalewajko, "Coupling of infrared radiation to intersubband transitions in multiple quantum wells: The effective medium approach" (to be published).
6. H.C. Liu (unpablished).
7. R.F. Kazarinov and R.A. Suris. '"Possibility of electromagnetic waves in a semiconductor with a superlattices", *Fiz. Tech. Polupr.* **5**, 797–800 (1971).
8. M. Helm, P. England, E. Colas, F DeRossa, and S.J. Allen, "Intersubband emission from semiconductor superlattices excited by sequential tunneling", *Phys. Rev. Lett.* **63**, 74–77 (1989).
9. J. Faist, F. Capasso, D.L. Sivco, C. Sirtiri, A. Hutinson, and A.Y. Cho, "Quantum cascade laser", *Science* **264**, 553–556 (1994).
10. C. Sirtori, F. Capasso, J. Faist, A.Y. Cho, P. Collot, V. Berger, and J. Nagle, "Mid-ir intersubband quantum cascade lasers", *Proc. SPIE* (in press).
11. C. Sirtori, A. Tredicucci, F. Capasso, J. Faist, D.L. Sivco, A.L. Huttison, and A.Y. Cho, "Dual-wavelength emission from optically cascaded intersubband transitions", *Optics Lett.* **23**, 463–465 (1998).

